Crystal structures and inhibitor binding in the octameric flavoenzyme vanillyl-alcohol oxidase

Mattevi, Andrea; Fraaije, Marco W.; Mozzarelli, Andrea; Olivi, Luca; Coda, Alessandro; Berkel, Willem J.H. van

Published in:
Structure

DOI:
10.1016/S0969-2126(97)00245-1

Publication date:
1997

Crystal structures and inhibitor binding in the octameric flavoenzyme vanillyl-alcohol oxidase: the shape of the active-site cavity controls substrate specificity

Andrea Mattevi[1]*, Marco W Fraaije[2], Andrea Mozzarelli[3], Luca Olivi[4], Alessandro Coda[1] and Willem JH van Berkel[2]

Background: Lignin degradation leads to the formation of a broad spectrum of aromatic molecules that can be used by various fungal micro-organisms as their sole source of carbon. When grown on phenolic compounds, *Penicillium simplicissimum* induces the strong expression of a flavin-containing vanillyl-alcohol oxidase (VAO). The enzyme catalyses the oxidation of a vast array of substrates, ranging from aromatic amines to 4-alkylphenols. VAO is a member of a novel class of widely distributed oxidoreductases, which use flavin adenine dinucleotide (FAD) as a cofactor covalently bound to the protein. We have carried out the determination of the structure of VAO in order to shed light on the most interesting features of these novel oxidoreductases, such as the functional significance of covalent flavinylation and the mechanism of catalysis.

Results: The crystal structure of VAO has been determined in the native state and in complexes with four inhibitors. The enzyme is an octamer with 42 symmetry; the inhibitors bind in a hydrophobic, elongated cavity on the *si* side of the flavin molecule. Three residues, Tyr108, Tyr503 and Arg504 form an anion-binding subsite, which stabilises the phenolate form of the substrate. The structure of VAO complexed with the inhibitor 4-(1-heptenyl)phenol shows that the catalytic cavity is completely filled by the inhibitor, explaining why alkylphenols bearing aliphatic substituents longer than seven carbon atoms do not bind to the enzyme.

Conclusions: The shape of the active-site cavity controls substrate specificity by providing a 'size exclusion mechanism'. Inside the cavity, the substrate aromatic ring is positioned at an angle of 18° to the flavin ring. This arrangement is ideally suited for a hydride transfer reaction, which is further facilitated by substrate deprotonation. Burying the substrate beneath the protein surface is a recurrent strategy, common to many flavoenzymes that effect substrate oxidation or reduction via hydride transfer.

Addresses: [1]Department of Genetics & Microbiology, University of Pavia, via Abbiategrasso 207, 27100 Pavia, Italy, [2]Department of Biochemistry, Agricultural University, Dreijenlaan 3NL-6703 HA Wageningen, The Netherlands, [3]Institute of Biochemical Sciences, University of Parma, Viale delle Scienze, 43100 Parma, Italy and [4]X-ray Diffraction Beam Line, ELETTRA, Padriciano 99, 34012 Trieste, Italy.

*Corresponding author.
E-mail: MATTEVI@IPVGEN.UNIPV.IT

Key words: catalysis, cavity, FAD, X-ray crystallography

Received: 8 April 1997
Revisions requested: 28 May 1997
Revisions received: 12 June 1997
Accepted: 17 June 1997

Structure 15 July 1997, 5:907–920
http://biomednet.com/elecref/0969212600500907

Introduction

Lignin is the most abundant aromatic biopolymer on earth. In addition to conferring strength to plants, it provides a barrier against microbial attack and protects cellulose from hydrolysis. Among the relatively few organisms able to degrade lignin, white rot fungi are particularly efficient in carrying out the lignolytic process, which has been described as an 'enzymatic combustion' [1] due to the broad substrate specificity of the enzymes involved. Lignin degradation results in the production of various aromatic molecules, which can be used as source of carbon by soil inhabitants, such as several basiodiomycetes and ascomycetes. The aryl alcohol oxidases, a wide group of flavine adenine dinucleotide (FAD)-dependent enzymes which produce hydrogen peroxide through the oxidation of their aromatic substrates, are crucial for the degradation of the secondary metabolites derived from the lignolytic process [2]. Recently, we have isolated from the ascomycete *Penicillium simplicissimum* a novel type of aryl alcohol oxidase, vanillyl-alcohol oxidase (VAO) [3,4], which consists of eight identical subunits each comprising 560 amino acids and a molecule of 8α-(N3-histidyl)-FAD as a covalently bound prosthetic group. A noticeable feature of VAO is its strikingly broad substrate specificity. In fact, besides the vanillyl-alcohol (4-hydroxy-3-methoxybenzyl alcohol) oxidation to vanillin (4-hydroxy-3-methoxybenzaldehyde; Figure 1a), VAO is able to carry out the oxidative demethylation of 4-(methoxymethyl)phenol to 4-hydroxybenzaldehyde (Figure 1b), the oxidative deamination of vanillylamine to vanillin and the conversion of eugenol (4-allyl-2-methoxyphenol) to coniferyl alcohol (4-hydroxy-3-methoxycynnamyl alcohol) [4]. In spite of this wide spectrum of activity, two features common to the VAO

Figure 1

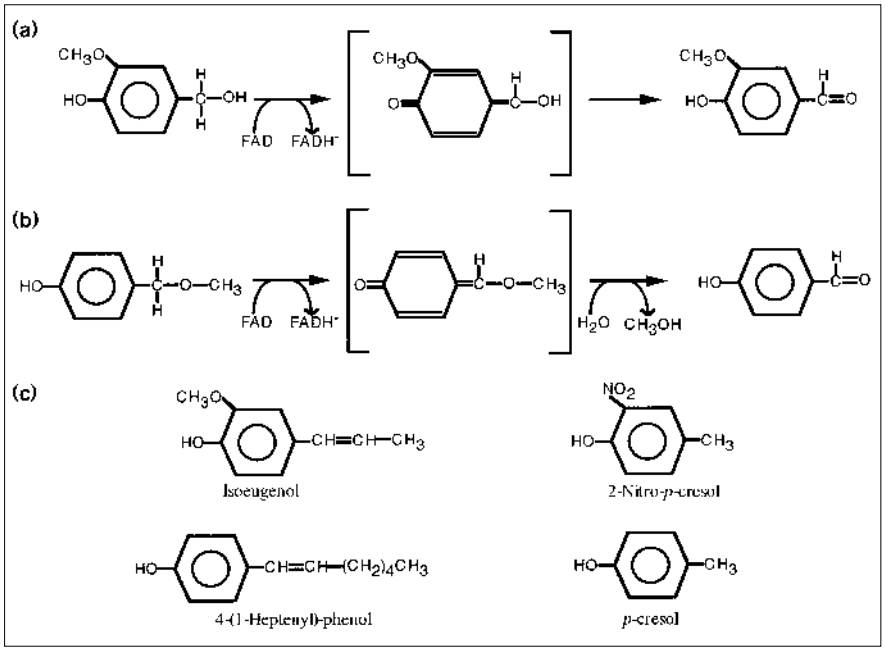

Substrate and inhibitors of VAO. Examples of different reactions catalysed by VAO are: (a) the oxidation of vanillyl-alcohol to vanillin and (b) the oxidative demethylation of 4-(methoxymethyl)phenol. The catalysed reactions are thought to proceed through a *p*-quinone methide intermediate shown in square brackets. The reduced FAD is reoxidised by molecular oxygen (not shown). (c) The chemical structures of the competitive inhibitors and active-site ligands employed for the crystallographic analysis.

catalysed reactions can be identified: the reaction is thought to be initiated by the oxidation of the substrate Cα atom resulting in a *p*-quinone methide intermediate (Figure 1b); and the reduced flavin is reoxidised by molecular oxygen, with the production of a hydrogen peroxide molecule.

A thorough characterisation of the VAO substrate specificity has revealed that the enzyme can bind aromatic compounds bearing aliphatic groups of variable size, ranging from a small methyl group to an aliphatic chain of up to seven carbon atoms [5]. Moreover, the *ortho* substituent can be either a H, OH or OCH_3 group, whereas a hydroxyl substituent *para* to the aliphatic chain is strictly required for binding [4]. This ability of VAO to convert a wide range of substrates has led to the speculation that *in vivo* the enzyme may be involved in the degradation of several metabolites. The fact that the expression of VAO is strongly induced by the presence of 4-(methoxymethyl)phenol in the growth medium, however, suggests that the main physiological role [6] of the enzyme is that of degrading this compound, leading to the production of methanol and 4-hydroxybenzaldehyde (Figure 1b).

Analysis of the primary sequence of VAO (JAE Benen *et al.*, personal communication) has revealed that the enzyme belongs to a recently discovered family of FAD-dependent oxidoreductases [7,8]. The other known members of this family are D-lactate dehydrogenase, 6-hydroxy-D-nicotine oxidase, L-gulono-γ-lactone oxidase and *p*-cresol methylhydroxylase (PCMH). These proteins, which catalyse a wide range of chemical reactions, share a weak sequence homology. PCMH is a well-characterised flavocytochrome whose three-dimensional structure has been reported [9, 10]. Despite a 26% sequence identity (JAE Benen *et al.*, personal communication), PCMH differs from VAO in two major aspects: in PCMH the FAD cofactor is covalently bound to a tyrosine rather than to a histidine residue; and the reduced cofactor is reoxidised by electron transfer to the heme group and not by molecular oxygen as in VAO [9].

The covalent linkage of the FAD cofactor to the protein is a feature common to most members of the VAO-related oxidoreductase family [7]. Although covalent flavinylation has been observed in many flavoproteins, the mechanism of formation and the functional role of the covalent bond are poorly understood [10,11]. In this respect, the VAO-related oxidoreductases are particularly attractive for study as they portray different types of flavinylation, such as the 8α-(O-tyrosyl)-FAD of PCMH, the 8α-(N1-histidyl)-FAD of L-gulono-γ-lactone oxidase and the 8α-(N3-histidyl)-FAD of VAO and 6-hydroxy-D-nicotine oxidase.

In the framework of a project devoted to the analysis of flavoenzyme structure and function [12,13], we describe the crystal structure of VAO in the native state and in complexes formed with the competitive inhibitors ioseugenol (2-methoxy-4-(1-propenyl)phenol), *p*-cresol (4-methyl-phenol), 2-nitro-*p*-cresol, and with the reaction product 4-(1-heptenyl)phenol (Figure 1c). The crystallographic analysis has been accompanied by a microspectrophotometric investigation, aimed at the precise determination of the FAD redox state in the various crystal complexes. These

Table 1

Refinement statistics.

VAO complex	Native	*p*-Cresol	Isoeugenol	2-Nitro-*p*-cresol	Heptenyl-phenol
Resolution (Å)*	10.0–2.5	100.0–2.7	100.0–2.8	100.0–3.1	100.0–3.3
R_{factor} (%)	22.1	22.2	21.5	20.6	22.5
R_{free} (%) (1000 reflections)	29.7	29.3	29.5	24.9	26.8
Number of protein atoms†	2×4408	2×4452	2×4455	2×4455	2×4458
Number of water molecules	320	107	38	0	0
Rmsd from ideal values‡					
bond lengths (Å)	0.016	0.015	0.017	0.006	0.010
bond angles (°)	3.3	3.5	3.1	2.2	2.5
trigonal atoms (Å)	0.010	0.008	0.011	0.006	0.008
planar groups (Å)	0.009	0.009	0.009	0.006	0.006
non bonded atoms (Å)	0.047	0.065	0.064	0.030	0.039
ΔB bonded atoms (Å^2)	7.4	7.2	7.0	8.4	8.4

*All measured reflections were used for refinement (no σ cut-off). †Refinement was carried out with strict noncrystallographic symmetry constraints (two identical subunits); in all structures, the N-terminal residues (1–5) were disordered and not visible in the electron-density maps. Moreover, in the native structure residues 42–46 have poorly defined density and were not included in the final model. ‡The root mean square deviation (rmsd) from ideal values were calculated using the program TNT [35].

studies are the first step towards the characterisation of the most interesting features of VAO, such as the mechanism and functional role of the covalent flavinylation, the mechanism of FAD-mediated substrate oxidation and the possibility of exploiting the enzyme for the synthesis of compounds of industrial relevance [14]. In this regard, it is of note that the gene encoding VAO has been cloned (JAE Benen *et al.*, personal communication) paving the way to protein engineering studies.

Results and discussion

X-ray analysis

The three-dimensional structure of native VAO has been determined at 2.5 Å resolution using a combination of molecular replacement, isomorphous replacement and density modification techniques. A key step in the structure determination was the application of a phase refinement procedure in which the electron-density maps calculated with data collected at room temperature and at 100K were averaged. In this way, the phase error was decreased from 72° to 51°. The refined native structure (Table 1) has been used as an initial model for the refinement of four enzyme–ligand complexes. In all cases, the electron-density maps allowed an unambiguous location of the ligand within the enzyme active site. Inhibitor binding did not induce any significant conformational change, with root mean square (rms) deviations from all Cα atoms of the native structure of 0.41 Å, 0.39 Å, 0.37 Å and 0.37 Å for the VAO–2-nitro-*p*-cresol, VAO–*p*-cresol, VAO–isoeugenol and VAO–4-(1-heptenyl)phenol complexes, respectively. For the description of the overall structure, we shall refer to the native enzyme model in view of the higher resolution of the relative diffraction data.

Overall structure

Each VAO subunit comprises two domains (Figures 2a and 2b). The larger domain (residues 6–270 and 500–560) forms the FAD-binding site and consists of one antiparallel and one mixed β sheet surrounded by six α helices. The smaller cap domain (residues 271–499) covers the FAD isoalloxazine ring and encompasses a large seven-stranded antiparallel β sheet flanked on both sides by a total of seven α-helical regions (Figure 2b). The overall structure of the VAO subunit closely resembles that of PCMH, as indicated by an rms deviation of 1.2 Å for 470 Cα atom pairs (31% sequence identity for the amino acids used in the superposition). An in-depth comparison between VAO and PCMH [10] must await the completion of the crystallographic refinement of the PCMH structure.

In addition to the similarity with PCMH, there are a few other lines of evidence to suggest that the folding topology of VAO is shared by other FAD-dependent enzymes. Firstly, PCMH and VAO are members of the family of FAD-dependent oxidoreductases which share a weak, but significant, sequence similarity; these enzymes are therefore likely to display structural similarities [7,8]. Secondly, the VAO folding topology resembles that of MurB, a flavoenzyme involved in the biosynthesis of the bacterial cell wall [15]. In particular, the FAD-binding domains of

Figure 2

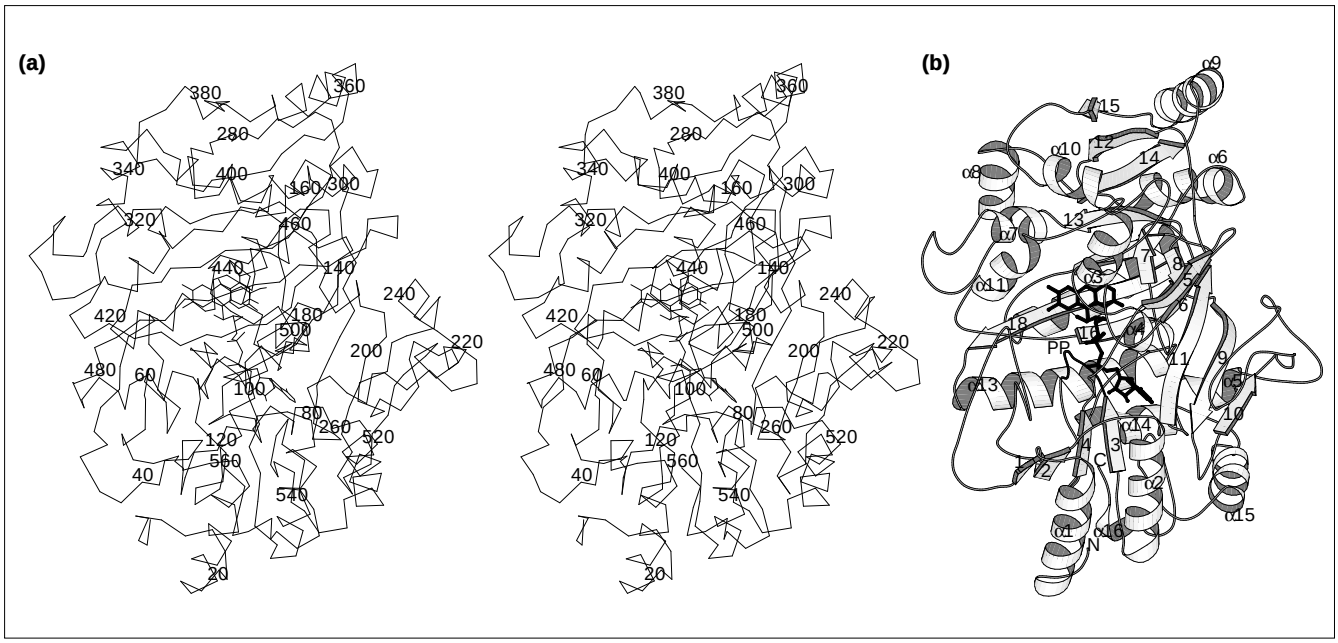

The structure of the VAO subunit. (a) Stereoview of the Cα trace of the subunit; every twentieth Cα atom is labelled with the residue number. The drawing was produced using the coordinates of the VAO–isoeugenol complex. (b) Ribbon drawing of the subunit. The β strands are labelled sequentially by numbers, whereas the α helices are indicated by α followed by a number. FAD is shown in ball-and-stick representation; the position of the PP loop (residues 99–110) is highlighted.

VAO and MurB can be superimposed with an rms deviation of 3.9 Å for 256 Cα atom pairs (13% sequence identity). This similarity, however, does not extend to the other parts of the structures, the cap domain of VAO being unrelated to the substrate-binding domain present in MurB [15]. Therefore, the FAD-binding domain observed in VAO may be viewed as a sort of 'cofactor-binding unit' employed by various flavoenzymes, otherwise differing in the rest of their three-dimensional structure.

In solution, VAO is an octamer of eight identical subunits. Analysis of the crystal packing reveals that this oligomeric arrangement is maintained in the tetragonal crystals used for structure determination. The octamer has 42 symmetry, with the molecular fourfold axis being coincident with the crystallographic c axis. The oligomer can be described as a tetramer of dimers (Figures 3a and 3b) in which each dimer is stabilised by extensive intersubunit contacts, as indicated by the burial of 18% (3950 Å^2) of the monomer accessible surface area upon dimer formation. In contrast to the strength of the monomer–monomer interactions, the dimer–dimer contact area is limited to a restricted number of residues. Upon octamer formation, only 5% (1200 Å^2) of the monomer accessible surface area becomes buried. This is in keeping with the observation that, in the presence of chaotropic agents, the octamer dissociates into dimers [16].

FAD binding

A cofactor molecule is bound by the FAD domain of each subunit (Figures 2a and 2b). Except for the ribose moiety, all cofactor atoms are solvent inaccessible, being involved in a number of interactions with the protein (Figure 4). A major role in FAD binding is played by residues 99–110, which form a coil region connecting β strands 3 and 4 (Figure 2b). This loop (called the 'PP loop' in Figure 2b) contributes to the binding of the adenine portion of FAD and compensates for the negative charge of the cofactor through the formation of hydrogen bonds between the backbone nitrogen atoms of residues Ser101, Ile102, Gly103, Arg104 and Asn105 and the pyrophosphate oxygen atoms (Figure 4).

VAO is the first enzyme of known structure in which the isoalloxazine ring is linked to the protein by a covalent bond between the flavin C8M atom and the Nε2 atom of His422 (Figures 4 and 5). The covalent linkage does not perturb the flavin conformation, which is planar. In addition to the covalent bond, the isoalloxazine ring forms several hydrogen bonds with the protein (Figures 4 and 5). In particular, two charged sidechains interact with the flavin ring: Arg504 and Asp170. Arg504 is engaged in hydrogen bond formation with the flavin O2 atom; as in many flavoenzymes [17], the proximity of a positive charge to the N1–C2=O2 locus stabilises the anionic form of the cofactor which is generated

Figure 3

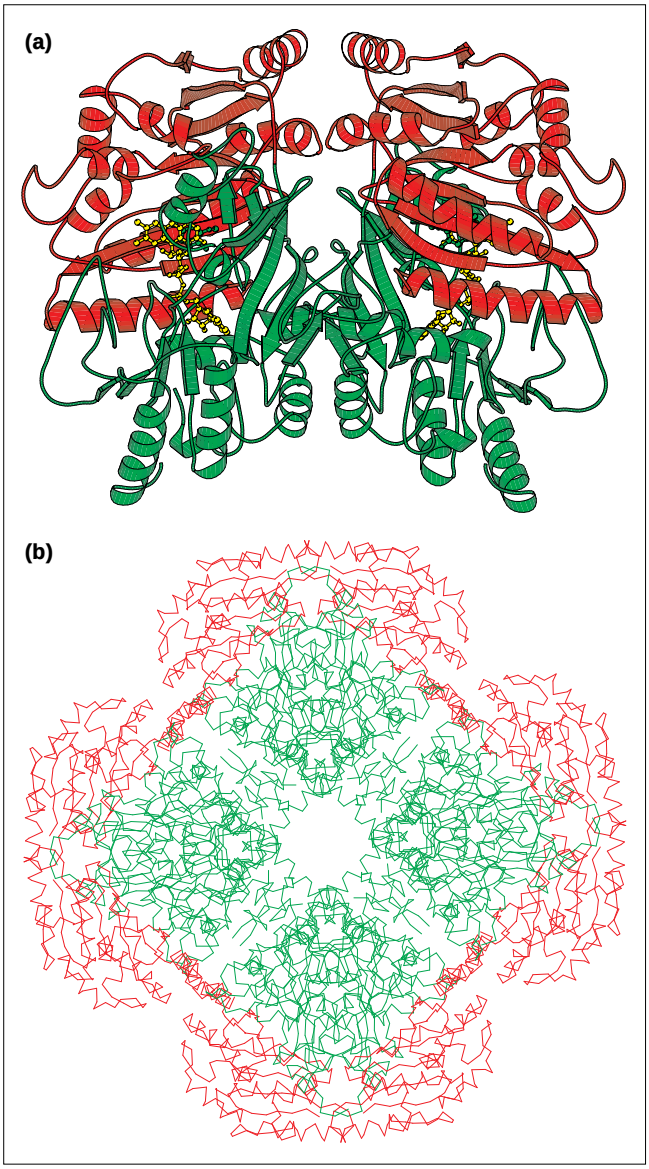

The quaternary structure of VAO. (a) The VAO dimer drawn with the FAD-binding domains in green and the cap domains in red; FAD is shown in yellow ball-and-stick representation. The molecular twofold axis is vertical; the orientation is the same as in Figure 2a. (b) Cα trace of the eight subunits forming the VAO octamer, viewed along the fourfold axis; the dimers are coloured as in (a).

upon reduction [3]. More unusual is the second interacting charged residue, Asp170, which is located only 3.5 Å from the flavin N5 position (Figure 4). It cannot be excluded that in the crystal structure Asp170 may be protonated, given the low pH (4.6) of the crystallisation medium. Asp170 is, however, within hydrogen-bonding distance of Arg398, whose positive charge should favour deprotonation of the aspartic acid carboxylic group. In particular, Asp170 should be ionised at the high pH values (around pH 10) at which VAO turnover is optimal for all investigated substrates [4,5]. The proximity of a negatively charged group to the N5 atom is intriguing, as in many flavin-dependent oxidoreductases of known structure the N5 atom is in contact with a hydrogen-bond donor rather than an acceptor [18]. The positioning of Asp170 is such that it could stabilise the reduced flavin by interacting with the protonated N5 atom of the reduced cofactor, thus increasing the FAD redox potential. The protonation state of Asp170, however, may change during catalysis (see below), making the role of this residue in the modulation of the cofactor redox properties even more enigmatic.

The electron-density maps of the native enzyme show a strong peak at ~3.5 Å from the *re* side of the flavin. We have interpreted this feature as due to a bound Cl^- ion held in position by interactions with the backbone nitrogen atoms of Asp170 and Leu171 (Figure 5). This interpretation is supported by the fact that Cl^- binds to VAO with a dissociation constant (K_d) of 140 μM. Remarkably, in spite of the vicinity to the cofactor, Cl^- binding has only a marginal effect on enzyme activity, slightly decreasing V_{max} to 80% of its normal value.

Catalytic centre

The VAO catalytic centre (Figure 5) is located on the *si* side of the flavin ring and is delimited mainly by hydrophobic and aromatic residues. In the native enzyme, the active site is occupied by a number of ordered solvent molecules. Furthermore, an electron-density peak, too large to be accounted for by a water molecule, has been tentatively assigned to an acetate ion, which is located 4.1 Å from the flavin ring and is hydrogen bonded to the sidechains of Tyr108, Tyr503 and Arg504 (Figure 5).

A surprising feature emerging from the analysis of the three-dimensional structure of VAO is that the active site is completely solvent inaccessible. In fact, the shape of the catalytic centre is that of a closed, elongated cavity having a volume [19] of approximately 200 $Å^3$ (Figure 6). Inspection of the protein structure does not suggest any obvious structural element, whose conformational change may allow substrate admission into the active site. In this context, it is remarkable that all the VAO–inhibitor complexes were generated by soaking experiments, indicating that the conformational changes required for substrate binding are tolerated by the crystal lattice.

VAO–isoeugenol and VAO–2-nitro-*p*-cresol complexes

Isoeugenol is one the best VAO inhibitors, having a dissociation constant K_d ranging from 15 μM (at pH 10) to 40 μM at pH 4 [4]. The electron-density map calculated with data collected from an isoeugenol soaked crystal has allowed us to unambiguously position the ligand within the active site (Figure 7). Only the γ carbon atom of the propenyl substituent (Figure 1c) is not well defined in

Figure 4

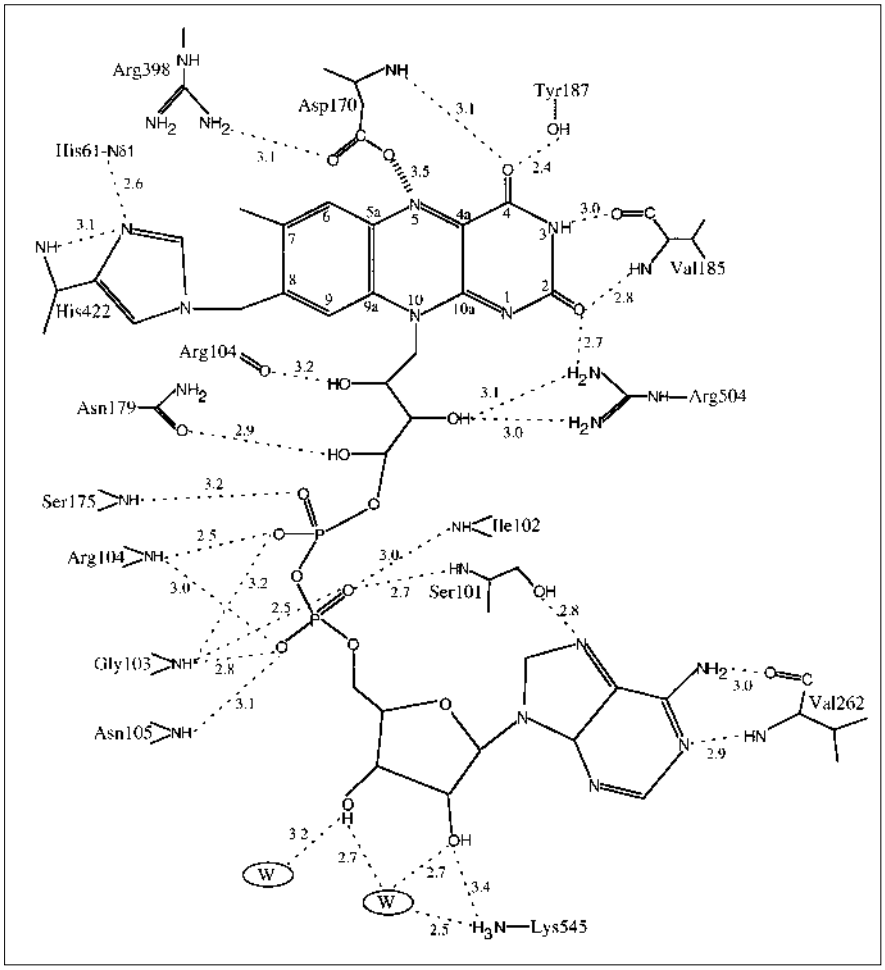

Schematic diagram of the protein–FAD interactions. Hydrogen bonds are indicated by dashed lines. The interatomic distances are shown in Å and refer to the native VAO structure. The Asp170–N5 contact is highlighted because of its particular relevance to the catalytic reaction.

density and was not included in the refined model. Isoeugenol binds with the aromatic ring stacking against the FAD pyrimidine ring at an angle of 18° with respect to the cofactor plane. The inhibitor fits snugly in the active site being in van der Waals contacts with the sidechains of Tyr108, Phe424 and Val185 (Figure 7). Moreover, the hydroxyl substituent is hydrogen bonded to Tyr503, Arg504 and Tyr108, whereas the propenyl group points towards Asp170 (Figure 7). The propenyl α carbon is located exactly above the flavin N5 position at a distance of 3.5 Å from the cofactor.

Characterisation of the substrate specificity properties of VAO have revealed that the hydroxyl substituent of the substrate *para* to the aliphatic chain is strictly required for binding and catalysis [4]. Moreover, the pK_a value of the ligand hydroxyl group is decreased by at least two units upon binding to the protein. For instance, the pK_a value of the enzyme-bound isoeugenol is lower than 6, suggesting that VAO preferentially binds the phenolate form of the inhibitor even at the low pH value (4.6) of the crystallisation medium. Inspection of the three-dimensional structure provides a rationale for the enzymes ability to induce such a lowering of the pK_a value. The hydroxyl group of the ligand is located at the heart of a network of interactions which involve a strong hydrogen bond with Tyr503 (hydrogen bond distance of 2.4 Å) and two weak hydrogen bonds with Tyr108 and Arg504 (hydrogen bond distance of 3.4 Å; Figure 7). In particular, the positively charged arginine sidechain may help to compensate for the negative charge of the phenolate ligand. In this respect, it is remarkable that the position of the isoeugenol hydroxyl atom overlaps that of the carboxylate group of the putative acetate ligand, supposedly bound in the native enzyme active site (Figure 5). All these observations strengthen the view that the clustering of Tyr503, Tyr108 and Arg504 forms a sort of anion hole, instrumental to substrate deprotonation.

2-Nitro-*p*-cresol is a competitive inhibitor of VAO (K_d = 40 μM at pH 5.5). X-ray analysis reveals that the binding mode of 2-nitro-*p*-cresol is virtually identical to that of isoeugenol, with the 2-nitro substituent located in the

Figure 5

Stereoview drawing of the active-site residues and isoalloxazine ring in the native VAO structure. The putative acetate ion (see text) is shown in black ball-and-stick form; hydrogen bonds are represented by dashed lines. With respect to Figure 2a, the molecule has been rotated by 30° about the vertical axis.

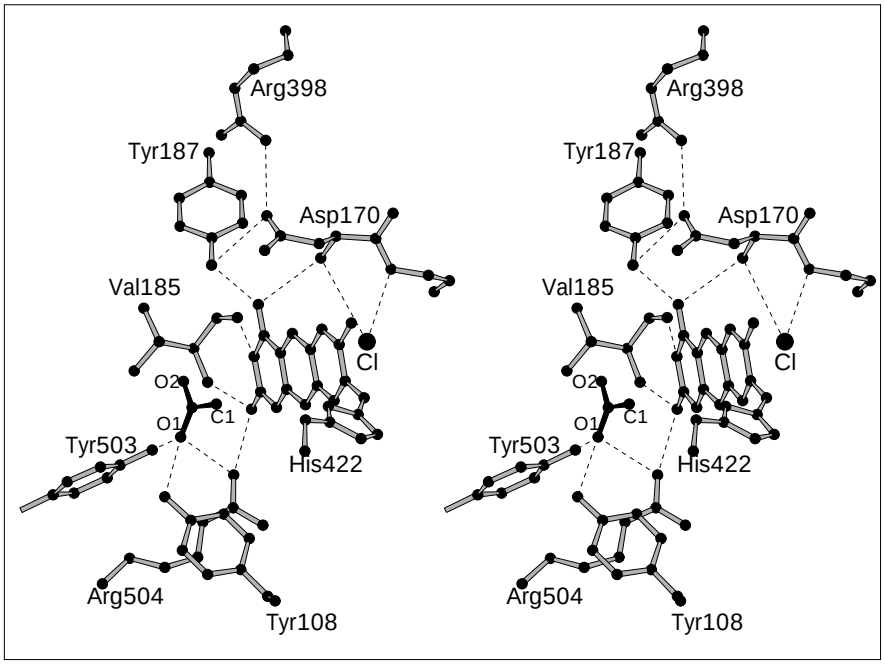

same place as the isoeugenol methoxy group. Remarkably, in both cases inhibitor binding does not cause any change in the active site. When the residues within 5 Å of the flavin N5 atom are considered, the rms deviation from the native enzyme is 0.33 Å and 0.43 Å for the VAO–isoeugenol and VAO–2-nitro-*p*-cresol complexes, respectively. Thus, VAO is able to completely embed a ligand within the active site, without modifying the conformation of any of the catalytic residues.

VAO–4-(1-heptenyl)phenol complex

Even in the presence of isoeugenol, the catalytic centre displays a residual void, having a volume of 45 Å^3 located in the proximity of Asp170 (Figure 7). This observation prompted us to investigate the binding and reactivity of substrates bearing aliphatic substituents of increasing length [5]. These studies revealed that phenol derivatives with an aliphatic chain of up to seven carbon atoms are substrates of VAO, while the catalytic activity completely

Figure 6

Stereoview drawing of the binding of 4-(1-heptenyl)phenol (shown in black) to VAO. The surface of the active-site cavity is shown in chicken wire representation. The surface was calculated [19] by omitting the 4-(1-heptenyl)phenol ligand from the model. For clarity, the label of Asp170 (positioned behind the heptenyl group) has not been drawn.

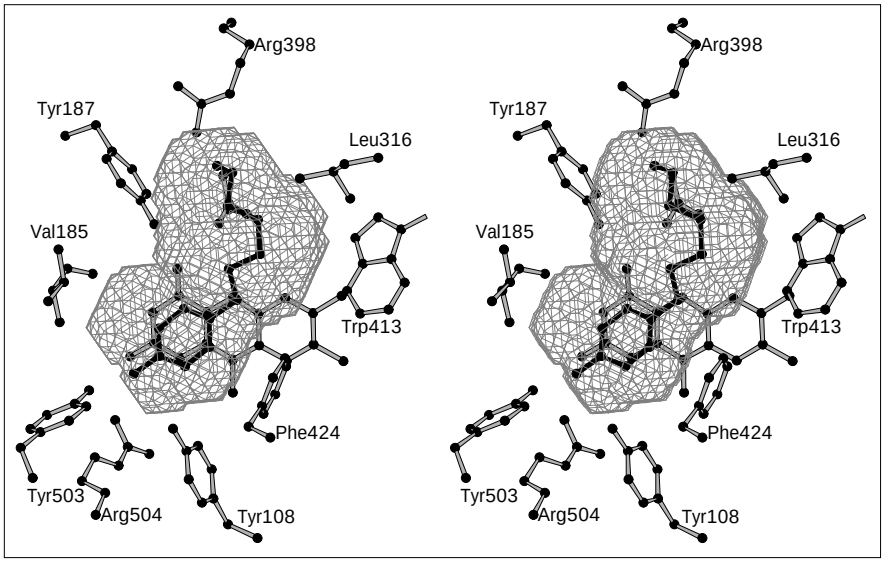

Figure 7

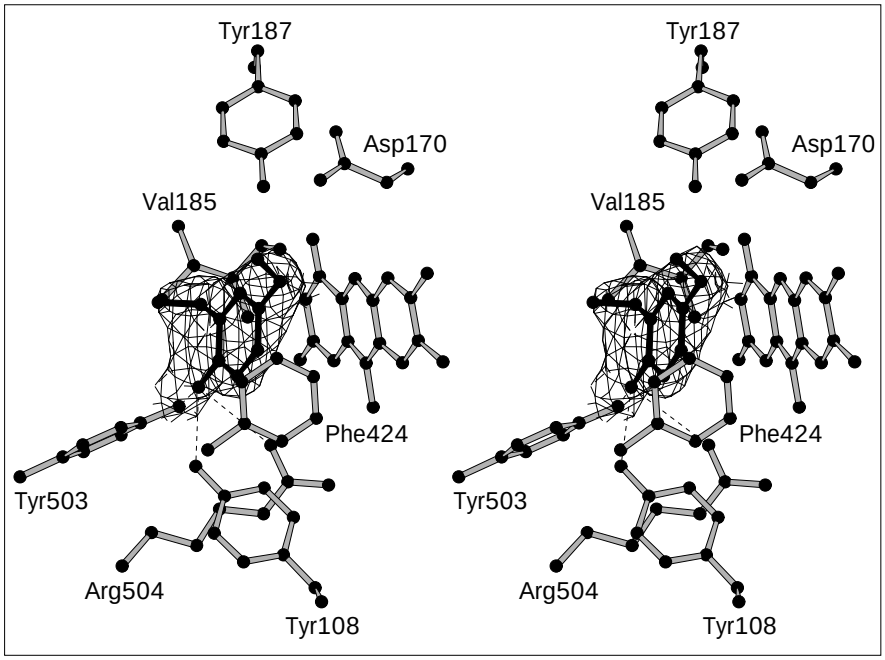

Stereoview drawing of the $2F_o–F_c$ map for isoeugenol bound to VAO; the contour level is 1σ. The isoeugenol atoms were omitted from the phase calculation, but otherwise the coordinates of the final model were used for structure-factor calculation. The dashed lines outline the hydrogen bonds between the inhibitor and the protein. The orientation of the figure is the same as for Figure 5.

falls off with aliphatic substituents consisting of eight or more carbon atoms. In order to provide a structural explanation for such specificity properties, we have determined the structure of VAO in complex with 4-(1-heptenyl)-phenol (Figure 1c). This molecule binds with the heptenyl substituent pointing towards Arg398 and interacting with the sidechains of Tyr187, Asp170, Leu316 and Trp413 (Figure 6); no residual void is present in the active site, which is completely filled by the ligand. Moreover, despite its bulkiness, no significant conformational changes are induced by binding of heptenylphenol which, in analogy with isoeugenol and 2-nitro-*p*-cresol, is inaccessible to the solvent. Thus, the substrate specificity of VAO seems dictated by a 'size exclusion' mechanism, in which the rigidity of the active-site cavity poses a limit to the size of the aliphatic substituents. In this respect, the structure explains the inability of the enzyme to bind substrates bearing methoxy substituents at both *ortho* positions (i.e. 4-alkyl-2,6-dimethoxyphenols): the second methoxy group would collide against Phe424 and Ile468, thus preventing binding to the enzyme.

The VAO–*p*-cresol adduct

p-Cresol (Figure 1c) is a slowly catalysed substrate of VAO ($k'_{cat} = 0.01\ s^{-1}$) and its binding results in the stabilisation of an intermediate complex in which the flavin is reduced [5]. This fact is particularly noticeable because such a complex is stable in the presence of oxygen, which normally reoxidises the cofactor very quickly. Given these peculiar properties, the reactivity of *p*-cresol towards the crystalline enzyme was investigated by single crystal microspectrophotometry [20]. In agreement with solution studies, the spectra indicated that *p*-cresol binding results in the generation of a reduced form of the cofactor (Figure 8). Remarkably, the reaction proceeds very slowly, the FAD reduction being completed only after more than two days. Such a slow speed does not seem to be an intrinsic property related to the crystalline state, as dithionite is able to reduce the crystalline enzyme within a few seconds (Figure 8). Moreover, the differences between the spectra of the crystals soaked in dithionite and *p*-cresol, indicate substantial variations in the structure and environment of the reduced flavin. In particular, in the VAO–*p*-cresol complex, the absorption maximum around 370 nm and the residual absorbance at 439 nm are consistent with the formation of a covalent adduct between the substrate and the flavin N5 atom [21].

The electron-density map of the enzyme–*p*-cresol complex (Figure 9) revealed a strong peak located on the flavin *si* side and connected to the cofactor N5 position by a stretch of continuous density. In the light of the microspectrophotometric data, this feature was taken as an indication of a covalent adduct between the *p*-cresol methyl group and the flavin N5 atom (Figure 9). Adduct formation is associated with a distortion of the flavin ring, which deviates from planarity with an angle between the dimethylbenzene and the pyrimidine rings of 8.2°. Except for the flavin ring distortion, however, the presence of the adduct does not induce any conformational change in the active site, the rms difference from the catalytic residues of the native structure being 0.39 Å.

VAO is unusual in that it does not react with sulphite [3], which forms an N5 covalent adduct in most flavin-dependent oxidases [17]. The structure of the VAO–*p*-cresol complex shows that the N5-bound Cα atom is located 3.4 Å from Asp170. Thus, a sulphite group covalently bound to the flavin would make a highly unfavourable contact with Asp170, suggesting that electrostatic repulsion of this acidic sidechain is the likely cause of the unusual lack of reactivity of VAO towards sulphite.

The catalytic mechanism

Kinetic and spectroscopic studies [4,22] suggest that substrate oxidation proceeds via direct hydride transfer from the Cα atom to N5 of the FAD. Formation of the resulting *p*-quinone methide intermediate (Figure 1a) is thought to be facilitated by the preferential binding of the phenolate form of the substrate (pK_a of isoeugenol <6). The VAO three-dimensional structure is in excellent agreement with this proposal. The VAO–isoeugenol (Figure 7) and VAO–2-nitro-*p*-cresol complexes reveal that the enzyme achieves hydride transfer by positioning the ligand Cα atom 3.5 Å from N5. Moreover, the inhibitor hydroxyl oxygen is hydrogen bonded to three residues, Arg504, Tyr503 and Tyr108, which are ideally located to stabilise the phenolate negative charge (Figures 7 and 10). The propensity of these sidechains for binding anionic molecules is further underlined by the presence, in the native structure, of an acetate ion directly interacting with the phenolate-binding cluster (Figure 5).

Under anaerobic conditions, reaction with 4-(methoxymethyl)phenol leads to a stable reduced enzyme–*p*-quinone methide complex (Figure 10) [22]. Only after exposure to oxygen and consequent FAD reoxidation, is the reaction completed with the synthesis and release of the final oxidised product (Figure 10). The three-dimensional structures of VAO suggest that charge balancing between the flavin, the quinone intermediate and Arg504 may determine the sequence of the catalytic steps. In fact, in addition to the interaction with the phenolate oxygen, Arg504 is well positioned to stabilise a negative charge on the N1–C2=O2 locus of the anionic reduced cofactor (Figures 4 and 5). Flavin C2, however, is located ~4 Å from the expected position of the oxygen atom of the *p*-quinone methide molecule bound to the reduced enzyme (Figure 7). Therefore, in the reduced enzyme, electrostatic repulsion by the negative charge of the flavin C2 locus should prevent formation of the phenolate ion, thus stabilising the quinone form of the intermediate (Figure 10). On the contrary, upon flavin reoxidation, Arg504 is deprived of an anionic partner, triggering the development of a negative charge on the quinone oxygen atom (Figure 10). In this way, the electrophilicity of the methide carbon is increased, facilitating hydroxylation (as for the 4-(methoxymethyl)phenol; Figure 10) or deprotonation (as for vanillyl-alcohol; Figure 1a) of the intermediate, producing the final product.

Figure 8

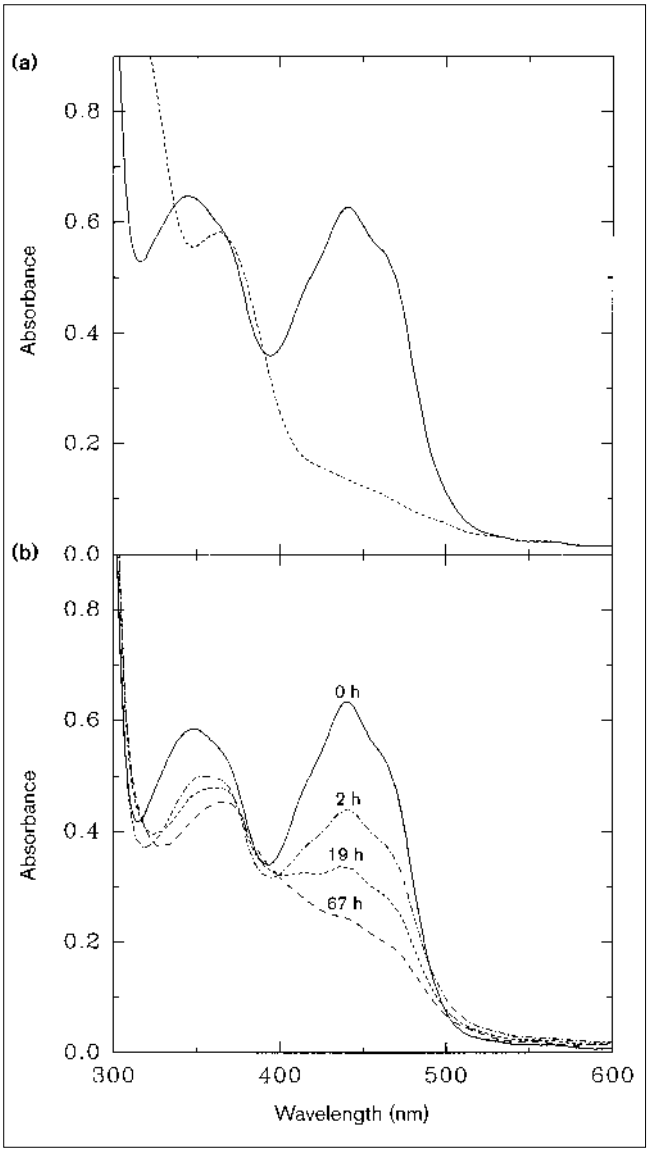

Polarised absorption spectra of VAO crystals. Polarised absorption spectra were recorded along two perpendicular directions on a crystal face that shows very weak bi-refringence. As the two spectra were very similar, only spectra recorded in one direction are presented. (a) Single crystal polarised absorption spectra of VAO crystals suspended in a solution containing 100 mM sodium acetate pH 4.6, 12% w/v PEG 4000 in absence (continuous line) and presence (dashed line) of sodium dithionite. The removal of dithionite led to the recovery of the oxidised enzyme (not shown). (b) Polarised absorption spectra of VAO crystals soaked in p-cresol were recorded 0, 2, 19 and 67 hours after starting the soaking experiment. After 67 hours, crystals were suspended in the same soaking solution but containing sodium dithionite; no spectral changes were observed (not shown). When these crystals were suspended in the standard storage solution (containing no p-cresol), spectra indicated a slow recovery of the oxidised enzyme.

In all the VAO structures investigated, the flavin N5 atom is within 3.4–3.6 Å of the sidechain of Asp170 (Figures 4 and

Figure 9

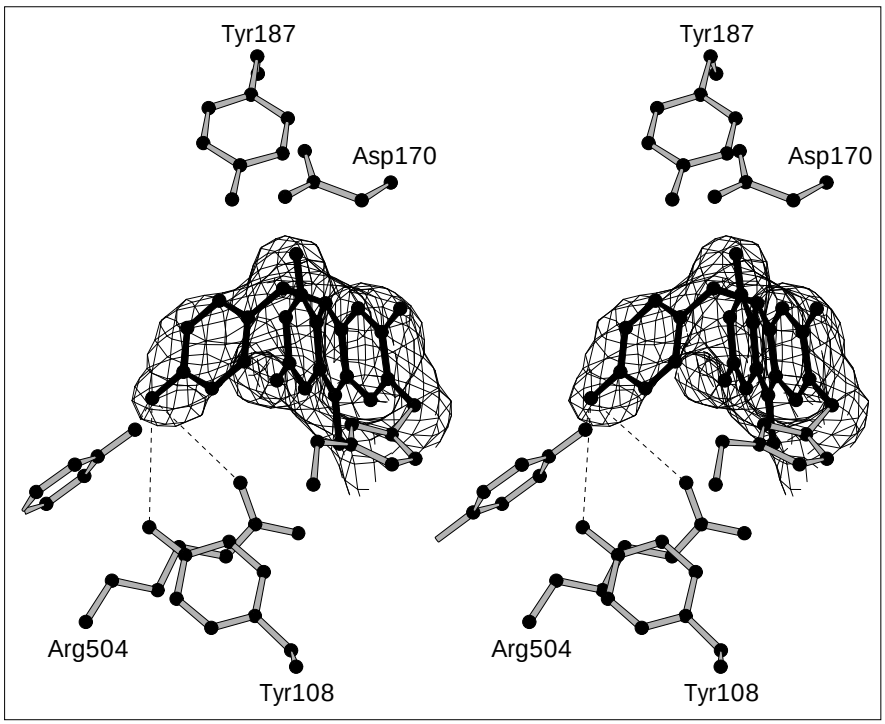

Stereoview drawing of the $2F_o–F_c$ map for the FAD–*p*-cresol adduct; the contour level is 1σ. The inhibitor and flavin atoms were omitted from phase calculation, but otherwise the coordinates of the final model were used for structure-factor calculation. The dashed lines depict the hydrogen bonds between *p*-cresol and the protein atoms.

7). This sidechain could function in catalysis as an active site base, either activating the water attacking the substrates undergoing hydroxylation (e.g. 4-(methoxymethyl)-phenol; Figure 10) or deprotonating the *p*-quinone methide intermediate in the case of substrates being dehydrogenated by the enzyme (e.g. vanillyl-alcohol; Figure 1a). It cannot, however, be excluded that the pK_a of Asp170 is shifted upwards by the enzyme, so that the sidechain is protonated,

Figure 10

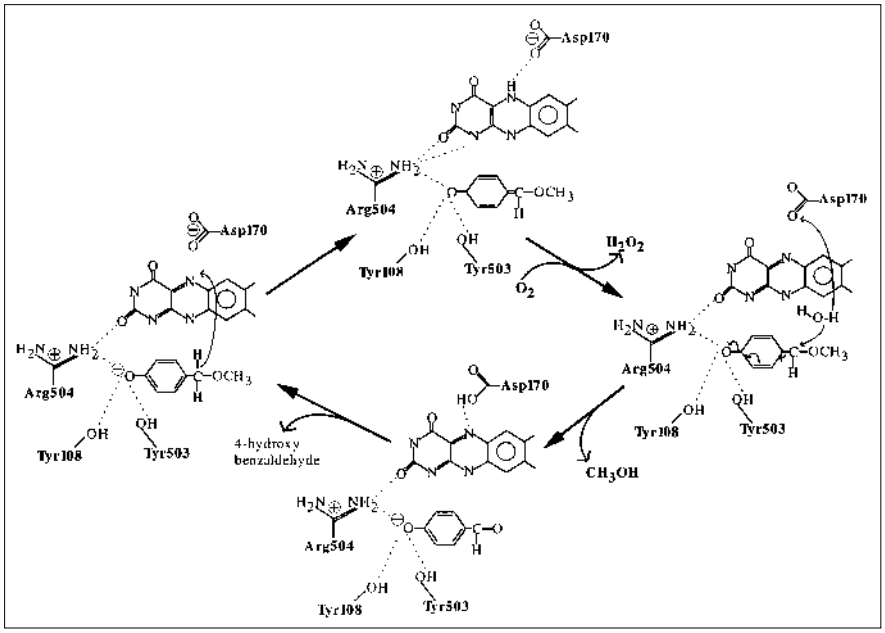

The reaction mechanism for the oxidation of 4-(methoxymethyl)phenol. In the first step, the substrate is oxidised via a direct hydride transfer from the substrate Cα atom to the N5 of flavin. The reduced cofactor is then reoxidised by molecular oxygen with the production of a hydrogen peroxide molecule. In the next step, the *p*-quinone-methoxymethide intermediate is hydroxylated by a water molecule, possibly activated by Asp170. The resulting 4-hydroxy-benzaldehyde and methanol products are released.

simply acting as hydrogen bond donor to flavin N5. It is evident that site-directed mutagenesis experiments need to be carried out in order to resolve the enigmatic role of this unusually located aspartate residue.

Reaction of the crystalline enzyme with *p*-cresol results in a stable covalent adduct between this substrate analogue and the reduced flavin (Figures 8 and 9). Stabilisation of the phenolate ion is expected to facilitate the nucleophilic attack of the methyl carbon on the flavin N5 position, leading to covalent adduct formation. Moreover, the side-chain of Asp170 could function as the base which abstracts the *p*-cresol α proton. Comparison between the VAO–isoeugenol and VAO–*p*-cresol complexes reveals an interesting difference in the orientation of the aromatic ring of the two ligands. The covalent bond forces *p*-cresol to be oriented towards the cofactor, making an angle of 34° with the flavin, whereas isoeugenol is less tilted with respect to FAD, with an angle of 18° between the inhibitor and isoalloxazine planes. This difference is relevant to the question as to why only *p*-cresol is able to form an adduct, whereas phenol compounds having either an ethyl or propyl substituent are regular VAO substrates [5]. A modelling experiment showed that, if the methyl group of *p*-cresol were replaced by an ethyl substituent (e.g. 4-ethylphenol), the additional methyl group would make an unfavourable contact (<2.4 Å) with either the flavin or Asp170 atoms. The same argument can be extended to also explain why 2-nitro-*p*-cresol does not form a covalent adduct: in this case, if the inhibitor plane were in the orientation required for adduct formation, the nitro substituent would make a short contact with Val185 (Figure 7). Thus, the steric restrictions imposed by the shape of the active-site cavity are a key factor for preventing enzyme inactivation through covalent adduct stabilisation.

Substrate burial: a recurrent theme in flavoenzyme catalysis

The VAO catalytic reaction takes place in the solvent-protected environment provided by the active-site cavity. This strategy fulfils different concurrent reaction goals: the cavity has a rather rigid architecture, limiting the size and structure of the active-site ligands; a solvent-protected environment is suited for binding the poorly soluble and hydrophobic VAO substrates; the low dielectric constant of the catalytic medium strengthens the electrostatic and polar interactions, which activate the substrate through phenolate formation; and a solvent inaccessible catalytic site is thought to effect the hydride transfer step leading to substrate oxidation. In this regard, it is fascinating that the strategy of embedding substrates and catalytic groups inside a solvent-protected site has been developed by a number of flavin-dependent oxidases and oxidoreductases, such as cholesterol oxidase [23], D-amino acid oxidase [12], dihydroorotate dehydrogenase [24] and medium acyl-CoA dehydrogenase [25]. All of these enzymes use this feature to catalyse substrate oxidation/reduction via an hydride transfer mechanism. In several of these enzymes (i.e. cholesterol oxidase, D-amino acid oxidase and dihydroorotate dehydrogenase) a loop changes conformation during the catalytic cycle, thus controlling the accessibility of the catalytic site. Analysis of the VAO structure, however, does not unambiguously reveal any structural element to act as an active-site gate. We shall address this problem by a combination of site-directed mutagenesis and structural studies.

Biological implications

Flavoenzymes are involved in a variety of chemical processes, ranging from simple redox reactions to DNA repair and light emission. In spite of this broad spectrum of activity, flavoenzymes can be grouped into a small number of classes, the members of which share various biochemical properties.

The oxidase class of flavoenzymes is characterised by the ability of the reduced flavin to react very rapidly with oxygen; the aryl-alcohol oxidases are members of this class of enzyme. Aryl-alcohol oxidases are fungal enzymes involved in the oxidation of aromatic compounds derived from the degradation of lignin. These enzymes typically display a broad substrate specificity, reflecting the highly heterogeneous composition of the lignin biopolymer. We report here the structure of vanillyl-alcohol oxidase (VAO), which is the first structure of a flavin-containing aryl-alcohol oxidase to be determined. VAO catalyses the oxidation of a vast array of phenolic compounds, ranging from various 4-alkylphenols to 4-hydroxybenzylalcohols and 4-hydroxybenzylamines. VAO consists of eight identical subunits assembled into an oligomer having 42 symmetry. Each subunit consists of two domains, which bind the flavin isoalloxazine ring at their interface. The folding topology of VAO closely resembles that of the flavoenzyme *p*-cresol methylhydroxylase and is likely to be shared by the members of a recently discovered family of evolutionary related flavin-containing oxidoreductases.

In VAO, the flavin ring is covalently bound to His422; covalent attachment is not associated to any distortion of the flavin, which is planar. This observation is relevant for the design of semisynthetic enzymes, made highly stable by the covalent linkage of the cofactor. Such semisynthetic proteins would be particularly suitable for biotechnological applications.

The crystal structures of four VAO–ligand complexes reveal the remarkable architecture of the active site, which comprises a completely solvent inaccessible, elongated cavity. The binding mode of the ligands within this catalytic cavity is compatible with substrate oxidation occurring via direct hydride transfer from the substrate

Cα atom to the flavin N5. Moreover, on the surface of the cavity, the sidechains of Tyr108, Tyr503 and Arg504 form an anion-binding site, that activates the substrate through the stabilisation of its phenolate form.

The burial of the substrate underneath the protein surface is an emerging theme, common to several flavin-dependent enzymes. The VAO structure reveals how this feature is instrumental to the control of the substrate specificity and effects the hydride transfer reaction leading to substrate oxidation.

Materials and methods

Crystallisation and crystal soaking

Crystals of VAO were obtained from a solution containing 6% w/v PEG 4000 0.1 M sodium acetate/HCl pH 4.6, using the hanging-drop vapour diffusion method. The crystals belong to space group I4 with cell dimensions a = b = 141 Å, c = 133 Å (Table 2). The asymmetric unit contains two VAO subunits related by a noncrystallographic axis perpendicular to the crystallographic c axis [26]. Preparation of the heavy-atom derivatives was hampered by the extreme sensitivity of the crystals towards heavy atom containing compounds. Only one suitable derivative was obtained, by soaking a crystal for 1 h in a solution containing 0.1 mM mercury acetate. The fragility of the VAO crystals probably relates to the fact that modification with *p*-mercuribenzoate leads to octamer dissociation [16].

In contrast to the sensitivity towards heavy-atom reagents, exposure to active-site ligands did not cause any damage to the crystals. Thus, all the VAO–ligand complexes could be prepared by soaking in ligand saturated solutions containing 10% w/v PEG 4000, 0.1 M sodium acetate/HCl pH 4.6.

Data collection

The data sets used for the single isomorphous replacement (SIR) phasing calculations and the analysis of the 4-(1-heptenyl)phenol and 2-nitro-*p*-cresol complexes were collected at room temperature using a RAXIS II imaging plate system equipped with a Rigaku 200 rotating anode CuKα X-ray source. The images were evaluated using a modified version of MOSFLM (program written by AGW Leslie), whereas the CCP4 suite of programs [27] was used for data reduction (Table 2). The data employed for refinement of the native, isoeugenol and *p*-cresol structures were collected at 100K using synchrotron radiation. Data for the native enzyme and *p*-cresol complex were measured at the X-ray diffraction beam line of ELETTRA (Trieste, Italy), while the data set for the VAO–isoeugenol complex was collected at the BW7B beam line of the EMBL outstation at DESY (Hamburg, Germany). In all cryocrystallographic experiments, 25% w/v PEG 400 was used as cryoprotectant. The data were integrated and scaled with the programs DENZO and SCALEPACK [28]. Freezing resulted in a substantial reduction of the unit cell parameters, the length of the a and b axes being decreased from 141 Å to about 128 Å (Table 2).

SIR phasing and molecular replacement

The data sets used for the SIR phasing calculations were collected at room temperature (Table 2). The difference Patterson map for the mercury derivative was solved using the Patterson superposition option of SHELXS-90 [29]. The six heavy-atom sites are close to the sidechains of Cys447, Cys470 and Cys495 of both subunits. The parameters of the mercury sites were refined with the program MLPHARE of the CCP4 package [27]. The resulting 3.2 Å SIR phases allowed the local twofold axis to be positioned in the unit cell by means of the 'real space translation function' option of GLRF [30]. An envelope around the protein could be calculated from a local correlation map [31]. The SIR phases were then improved by twofold averaging and solvent flattening using the program DM [32]. The resulting map, however, was uninterpretable.

While carrying out the structure determination, preliminary sequence data suggested an homology between VAO and PCMH [9]. Therefore, molecular replacement was attempted using a polyalanine search model derived from the partially refined structure of the PCMH subunit [10; FS Mathews, personal communication). A cross-rotation function calculated with the room temperature native data set resulted in two peaks at 3.3σ and 3.1σ above the mean [33]. A phased translation function [34] employing the SIR phases was then calculated. Both solutions of the cross-rotation function produced a peak at 10σ level (second peak at 5σ), making the interpretation of the phased translation function straightforward. The translated subunits were related by a

Table 2

Data collection and phasing statistics.

	Soaking time*	Cell axes a = b, c (Å)	Observations	Unique reflections	Resolution† (Å)	Completeness† (%)	R_{merge}‡ (%)	R_{iso}§ (%)	Phasing power#
Room temp									
Native		140.5, 132.9	86 175	20 541	3.2	98.1 (95.5)	10.4 (30.0)		
Mercury acetate	1 h	141.8, 133.5	48 825	19 231	3.2	90.7 (88.3)	8.2 (30.2)	31.4	1.4
2-Nitro-*p*-cresol	7 days	140.6, 132.5	43 741	21 522	3.1	94.3 (90.1)	6.2 (27.4)	14.0	
Heptenyl-phenol	1 month	141.0, 133.4	41 329	17 633	3.3	90.7 (86.1)	11.1 (33.9)	15.9	
100K									
Native		130.2, 133.5	330 030	38 274	2.5	98.9 (98.3)	8.8 (21.0)		
p-Cresol	7 days	128.8, 130.8	193 846	27 926	2.7	95.4 (84.2)	9.7 (31.2)	31.1	
Isoeugenol	7 days	128.4, 130.2	175 968	23 480	2.8	90.6 (83.1)	11.8 (32.2)	27.4	

Data collected at room temperature were measured on an in-house rotating anode, using an RAXIS II imaging plate. Data collected at 100K were measured either at ELETTRA or DESY synchrotron beam lines (see text) using a 180 mm diameter Hendrix-Lentfer imaging plate system. *The concentration of mercury acetate used for the soaking experiment was 0.2 mM; all other soaking experiments were carried out with ligand-saturated solutions. †The values relating to the highest resolution shell are given in brackets. ‡$R_{merge} = \Sigma|I_j - \langle I_j \rangle| / \Sigma \langle I_j \rangle$, where I_j is the intensity of an observation of reflection j and $\langle I_j \rangle$ is the average intensity for reflection j. §$R_{iso} = \Sigma||F_{PH}|-|F_P||/\Sigma|F_P|$, where F_{PH} is the structure-factor amplitude for the derivative or ligand-bound crystal and F_P is the structure-factor amplitude of a native crystal. The R_{iso} values were calculated with structure-factor amplitudes measured at the same temperature. #Phasing power = root mean square ($|F_H|/E$), where F_H is the calculated structure-factor amplitude due to the heavy atoms and E is the residual lack of closure error.

noncrystallographic symmetry (NCS) operator identical to that previously identified on the basis of the SIR phases, confirming the accuracy of the solution. The properly oriented and translated coordinates of the search model were then subjected to a few cycles of TNT [35] refinement. The resulting model was employed for a molecular replacement calculation using the 100K data set (Table 2). This procedure revealed that the operator relating the atomic coordinates of the 100K and room temperature structures correspond to a rotation defined by the polar angles $\kappa = 1.7°$, $\phi = 96.0°$, $\psi = 81.3°$ and a translation $T_x = -8.5$ Å, $T_y = -3.3$ Å, $T_z = 1.9$ Å.

Multicrystal density averaging

The large differences between the unit cell parameters of the room temperature and cryocooled crystals (Table 2) raised the possibility of treating them as two different crystal forms in a multicrystal density averaging procedure [36]. For this purpose, a protein envelope was defined on the basis of the PCMH coordinates, whereas the starting electron-density maps were derived from the SIR phases. The multicrystal averaging calculations were performed with the program DMMULTI [32] and resulted in a clearly interpretable map. In particularl, taking as reference the refined model phases, the mean error of the multicrystal averaged phases is 51°, which is 21° lower than the 72° error of the SIR twofold averaged phases. It must be stressed that the PCMH coordinates were employed for envelope definition but not for phase calculation, so that the multicrystal averaged maps were completely free of model bias. Freezing did not cause any significant change in the three-dimensional structure despite the large change in the unit cell parameters. In fact, after refinement of the atomic models (see below), the rms differences between the Ca atoms of the room temperature and low temperature structures (Tables 1 and 2) turn out to be smaller than 0.41 Å.

Crystallographic refinement

Least squares refinement was carried out with TNT [35] while the program O [37] was used for manual rebuilding of the model. Progress of the refinement was monitored by means of the free R factor [38], calculated from a set of randomly chosen 1000 reflections omitted from the least squares calculations. Strict NCS constraints were applied to all protein atoms, so that the two crystallographically independent subunits were kept identical. During refinement, the benzene ring and the pyrimidine ring of the flavin were restrained to be planar, but the central ring was allowed to bend or twist. This procedure was applied in order to allow the flavin to adopt a nonplanar conformation. Solvent molecules were included if they had suitable stereochemistry, after inspection of the difference electron-density maps (Table 1). In all investigated complexes, strong and well-defined density peaks allowed modelling of the active-site ligands (Figures 7 and 9). Only in the case of the VAO–isoeugenol complex, the third carbon atom of the propenyl chain (Figure 1c) was not well-defined in the density. This probably reflects the presence of a mixture of *cis* and *trans* isomers in the soaking solution , which both bind to the enzyme [4].

The refinement statistics are reported in Table 1. Out of 560 residues of each subunit, only the N-terminal five residues lack continuous density. In the native structure, residues 42–46 are not well defined in density and were not included in the final model. PROCHECK analysis shows that all refined models have stereochemical parameters well within the normal values found in protein structures (Table 1). The Ramachandran plot shows no residues in the disallowed regions, while 95% of the amino acids fall in the core regions defined by Kleywegt and Jones [39].

Atomic superpositions and model analysis were carried out using programs of the CCP4 package [27]. The drawings were generated with the program MOLSCRIPT [40]. The program VOIDOO [19] was employed for detection of cavities within the structure.

Microspectrophotometric studies and Cl^- binding

Single crystal absorption spectra [20] were obtained using a Zeiss MPM800 microspectrophotometer, with crystals in their soaking solution placed in a flow cell with quartz windows. Care was taken to carry out the spectrophotometric experiments in the same conditions employed for the preparation of the crystals used in the data collection. The dissociation constant and the effect of Cl^- on the enzyme activity were measured by spectrophotometric assays, as described [4,5].

Accession numbers

The atomic coordinates have been deposited with the Protein Data Bank. The accession codes are 1VAO (native enzyme), 2VAO (VAO–isoeugenol), 1AHU (VAO–*p*-cresol), 1AHV (VAO–nitro-*p*-cresol) and 1AHZ (VAO–4-(1-heptenyl)phenol).

Acknowledgements

We thank FS Mathews (Washington University, St. Louis) for providing us with the PCMH coordinates and J Visser and JAE Benen (Wageningen University) for the VAO amino acid sequence. We are indebted to all members of the Pavia protein crystallography group for a number of useful suggestions throughout the development of the project. The supervision of the EMBL/DESY staff during synchrotron data collection is gratefully acknowledged. This research was supported by a grant from the Consiglio Nazionale delle Ricerche (Contract n° 9502989CT14) to A.M.. We thank the European Union for support at the EMBL/DESY, through Human Capital Mobility Program to Large Scale Installations Project, Contract CHGE-CT93-0040.

References

1. Kirk, T.K. & Farrell, R.L. (1987). Enzymatic "combustion": the microbial degradation of lignin. *Annu. Rev. Microbiol.* **41**, 465–505.
2. De Jong, E., Field, J.A. & de Bont, J.A.M. (1994). Aryl alcohols in the physiology of ligninolytic fungi. *FEMS Microbiol. Rev.* **13**, 153–188.
3. De Jong, E., van Berkel, W.JH., van der Zwan, R.P. & de Bont, J.A.M. (1992). Purification and characterization of flavin-dependent vanillyl-alcohol oxidase from *Penicillium simplicissimum*. *Eur. J. Biochem.* **208**, 651–657.
4. Fraaije, M.W., Veeger, C. & van Berkel, W.JH. (1995). Substrate specificity of flavin-dependent vanillyl-alcohol oxidase from *Penicillium simplicissimum*. *Eur. J. Biochem.* **234**, 271–277.
5. Fraaije, M.W., Drijfhout, F., Meulenbeld, G.H., van Berkel, W.J.H. & Mattevi, A. (1997). Vanillyl-alcohol oxidase from *Penicillium simplicissimum*: reactivity with *p*-cresol and preliminary structural analysis. In *Flavoenzymes and Flavoproteins 1996 XII.* (Stevenson, K., Massey, V. & Williams, C.H., Jr., eds), University Press, Calgary, in press.
6. Fraaije, M.W., Pikkemaat, M. & van Berkel, W.J.H. (1997). Enigmatic gratuitous induction of the covalent flavoprotein vanillyl-alcohol oxidase in *Penicillium simplicissimum*. *Appl. Environ. Microbiol.* **63**, 435–439.
7. Mushegian, A.R. & Koonin, E.V. (1995). A putative FAD-binding domain in a distinct group of oxidases including a protein involved in plant development. *Protein Sci.* **4**, 1243–1244.
8. Murzin, A.G. (1996). Structural classification of proteins: new superfamilies. *Curr. Opin. Struct. Biol.* **6**, 386–394.
9. Mathews, F.S., Chen, Z., Bellamy, H.D. & McIntire, W.S. (1991). The three-dimensional structure of p-cresol methylhydroxylase (flavocytochrome c) from *Pseudomonas putida* at 3.0 Å resolution. *Biochemistry* **30**, 238–247.
10. Kim, J., *et al.*, & McIntire, W.S. (1995). The cytochrome subunit is necessary for covalent FAD attachment to the flavoprotein subunit of *p*-cresol methylhydroxylase. *J. Biol. Chem.* **270**, 31202–31209.
11. Stocker, A., Hecht, H.J. & Buckmann, A.F. (1996). Synthesis, characterisation and preliminary crystallographic data of N6-(6-carboamylhexyl)-FAD D-amino acid oxidase: a semisynthetic oxidase. *Eur. J. Biochem.* **238**, 519–528.
12. Mattevi, A., *et al.*, & Curti, B. (1996). Crystal structure of D-amino acid oxidase: a case of active site mirror-image convergent evolution with flavocytochrome b_2. *Proc. Natl. Acad. Sci. USA* **93**, 7496–7501.
13. Entsch, B. & van Berkel, W.J.H. (1995). Structure and mechanism of para-hydroxybenzoate hydroxylase. *FASEB J.* **9**, 476–483.
14. van Berkel, W.J.H., Fraajie, M.W., De Jong, E. (1997). Process for producing 4-hydroxycinnamyl alcohols. European Patent application 0710289B1.
15. Benson, T.E., Filman, D.J., Walsh, C.T. & Hogle, J.M. (1995). An enzyme–substrate complex involved in bacterial cell wall biosynthesis. *Nat. Struct. Biol.* **2**, 644–653.

16. Fraaije, M.W., Mattevi, A. & van Berkel, W.J.H. (1997). Mercuration of vanillyl-alcohol oxidase from *Penicillium simplicissimum* generates inactive dimers. *FEBS Lett.* 402, 33–35.
17. Ghisla, S. & Massey, V. (1989). Mechanisms of flavoprotein-catalyzed reactions. *Eur. J. Biochem.* 181, 1–17.
18. Fox, K.M. & Karplus, P.A. (1994). Old yellow enzyme at 2 Å resolution: overall structure, ligand binding, and comparison with related flavoproteins. *Structure* 2, 1089–1105.
19. Kleywegt, G.J. & Jones, T.A. (1994). Detection, delineation, measurement and display of cavities in macromolecular structures. *Acta Cryst. D* 50, 178–185.
20. Mozzarelli, A. & Rossi, G.L. (1996). Protein function in the crystal. *Annu. Rev. Biophys. Biomol. Struct.* 25, 343–365.
21. Ghisla, S., Massey, V. & Choong, Y.S. (1979). Covalent adducts of lactate oxidase. Photochemical formation and structure identification. *J. Biol. Chem.* 254, 10662–10669.
22. Fraaije, M.W. & van Berkel, W.J.H. (1997). Catalytic mechanism of the oxidative demethylation of 4-(methoxymethyl)phenol by vanillyl-alcohol oxidase. *J. Biol. Chem.*, in press.
23. Li, J., Vrielink, A., Brick, P. & Blow, D. (1993). Crystal structure of cholesterol oxidase complexed with a steroid substrate: implications for flavin adenine dinucleotide dependent alcohol oxidases. *Biochemistry* 32, 11507–11515.
24. Rowland, P., Nielsen, F.S., Jensen, K.F. & Larsen, S. (1997). The crystal structure of the flavin-containing enzyme dihydroorotate dehydrogenase A from *Lactococcus lactis*. *Structure* 5, 239–252.
25. Kim, J., Wang, M. & Paschke, R. (1993). Crystal structures of medium-chain acyl-CoA dehydrogenase from pig liver mitochondria with and without substrate. *Proc. Natl. Acad. Sci. USA* 90, 7523–7527.
26. Mattevi, A., Fraaije, M.W., Coda, A. & van Berkel, W.J.H. (1997). Crystallization and preliminary X-ray analysis of the flavoenzyme vanillyl-alcohol oxidase from *Penicillium simplicissimum*. *Proteins* 27, 601–603.
27. Collaborative Computational Project Number 4. (1994). The CCP4 suite: programs for protein crystallography. *Acta Cryst. D* 50, 760–767.
28. Otwinowski, Z. & Minor, W. (1993). *DENZO: A Film Processing Program for Macromolecular Crystallography.* Yale University, New Haven, CT.
29. Sheldrick, G.M. (1991). Heavy atom location using SHELXS-90. In *Isomorphous Replacement and Anomalous Scattering: Proceedings of the CCP4 Study Weekend 25–26 January 1991.* (Wolf, W., Evans, P.R. & Leslie, A.G.W. eds), pp. 23–38, SERC Daresbury Laboratory, Warrington, UK.
30. Tong, L. & Rossmann, M.G. (1990). The locked rotation function. *Acta Cryst. A* 46, 783–792.
31. Podjarny, A.D. & Rees, B. (1991). Density modification: theory and practice. In *Crystallographic Computing 5: from Chemistry to Biology.* (Moras, D., Podjarny, A.D. & Thierry, J.C., eds), pp. 361–372, Oxford University Press, Oxford, UK.
32. Cowtan, K.D. & Main, P. (1996). Phase combination and cross validation in iterated density-modification calculations. *Acta Cryst. D* 52, 43–48.
33. Navaza, J. (1994). AMORE: an automated procedure for molecular replacement. *Acta Cryst. A* 50, 157–163.
34. Read, R.J. & Schierbeek, A.J. (1988). A phased translation function. *J. Appl. Cryst.* 21, 490–495.
35. Tronrud, D.E., Ten Eyck, L.F. & Matthews, B.W. (1987). An efficient general-purpose least-squares refinement program for macromolecular structures. *Acta Cryst. A* 43, 489–501.
36. Rossmann, M.G. (1990). The molecular replacement method. *Acta Cryst. A* 46, 73–82.
37. Jones, T.A., Zou, J.Y., Cowan, S.W. & Kjeldgaard, M. (1991). Improved methods for building models in electron density maps and the location of errors in these models. *Acta Cryst. A* 47, 110–119.
38. Brünger, A.T. (1992). Free R value: a novel statistical quantity for assessing the accuracy of crystal structures. *Nature* 355, 472–475.
39. Kleywegt, G.J. & Jones, T.A. (1996). Phi/Psi-chology: Ramachandran revisited. *Structure* 4, 1395–1400.
40. Kraulis, P.J. (1991). MOLSCRIPT: a program to produce both detailed and schematic plots of protein structures. *J. Appl. Cryst.* 24, 946–950.